# Intramolecular Charge Transfer in Pyrromethene Laser Dyes: Photophysical Behaviour of PM650

**ARTICLE** *in* CHEMPHYSCHEM · DECEMBER 2004

Impact Factor: 3.42 · DOI: 10.1002/cphc.200400242 · Source: PubMed

CHEMPHYSCHEM

# Intramolecular Charge Transfer in Pyrromethene Laser Dyes: Photophysical Behaviour of PM650

F. López Arbeloa,* J. Bañuelos Prieto, V. Martínez Martínez, T. Arbeloa López, and I. López Arbeloa[a]

*Absorption and fluorescence (steady-state and time-correlated) techniques are used to study the photophysical characteristics of the pyrromethene 650 (PM650) dye. The presence of the cyano group at the 8 position considerably shifts the absorption and fluorescence bands to lower energies with respect to other related pyrromethene dyes; this is attributed to the strong electron-acceptor character of the cyano group, as is theoretically confirmed by quantum mechanical methods. The fluorescence properties of PM650 are intensively solvent-dependent. The fluorescence band is shifted to lower energies in polar/protic solutions, and the evolution of the corresponding wavelength with the solvent is analysed by a multicomponent linear regression. The fluorescence quantum yield and the lifetime strongly decrease in polar/protic solvents, which can be ascribed to an extra nonradiative deactivation, via an intramolecular charge-transfer state (ICT state), favoured in polar media.*

## Introduction

Since the discovery of dye lasers, these have been attractive sources of coherent tunable visible radiation, due to their operational advantages. Dye lasers can be pumped with a great variety of excitation sources and can emit in continuous wave and in pulsed forms. Owing to the broad gain bandwidth, they can generate ultrashort pulses and a wide tunability range.[1] Besides, dye lasers usually provide high-energy pulses and average powers. There is a great variety of laser dyes, which makes it possible to cover the entire visible region of the electromagnetic spectrum.[2] Due to the inherent characteristics of dye lasers, they have found applications in a wide range of fields, from medicine and industry to science (mainly in chemistry, physics and biology).[3]

The development of new active media for improving the lasing efficiency is focused on three different aspects: a) the modification of the dye structure, looking for more rigid structures that diminish the nonradiative processes and, hence, increase the fluorescence quantum yield;[4] b) the incorporation of the dye in new environments, such as polymers, sol-gel materials, nanocomposites,[5–9] looking for good solid-state dye lasers that provide more technological and commercial advantages (i.e., absence of bulky flow systems and solvents, better manageability and miniaturisation of the experimental setup) than those obtained in the liquid state and c) the synthesis of new laser dye families.

In this regard, Boyer and co-workers have developed a new family of laser dyes, pyrromethene-$BF_2$ complexes, the so-called PM dyes.[10,11] These dyes have strong absorption and fluorescence bands in the green–yellow region of the electromagnetic spectrum and present high fluorescence quantum yields.[12–16] They lase very efficiently,[11,17–19] even more than rhodamine dyes (which probably represent the best-known and most widely-used laser dyes),[20] owing to their high fluorescence capacity, very low probability of intersystem crossing and low triplet–triplet absorption in the laser emission wavelengths.[21–23] This interesting photophysical behaviour is a consequence of the quasiaromatic character of PM dyes.[24] Indeed, the introduction of linkage heteroatoms (B and F atoms) in the aromatic system blocks the flow of the $\pi$ electrons through the delocalised system, which reduces the spin–orbit coupling and, hence, the intersystem crossing to the triplet states.[4] Moreover, PM dyes yield a high photostability, which improves the operating lifetimes of these dyes as active media of tunable lasers.[25,26]

Previous works have demonstrated the existence of satisfactory correlations between the lasing characteristics (wavelength and efficiency) and the photophysics (fluorescence wavelength and quantum yield) of PM dyes by either modifying the molecular structure of the chromophore or the nature of the solvent.[27–29] For this reason, this Article is included in a series of papers focused to predict, from a photophysical point of view, the best environmental conditions to optimise the laser action of PM dyes.

It has been previously confirmed that the incorporation of different alkyl substituents (e.g., ethyl,[27] *t*-butyl[30] groups, see Figure 1) in the chromophore core modifies the photophysical and lasing characteristics of PM dyes to a low extent.[11,15,29] The photophysics of these PM analogues shows a light solvent dependence,[15,27,29] although polar/protic media are recom-

[a] *Prof. Dr. F. López Arbeloa, Dr. J. Bañuelos Prieto, V. Martínez Martínez, Dr. T. Arbeloa López, Prof. Dr. I. López Arbeloa*
*Departamento de Química Física*
*Universidad del País Vasco-EHU, Apartado 644*
*48080 Bilbao (Spain)*
*Fax: (+34) 946-013-500*
*E-mail: qfploarf@lg.ehu.es*

  DOI: 10.1002/cphc.200400242 

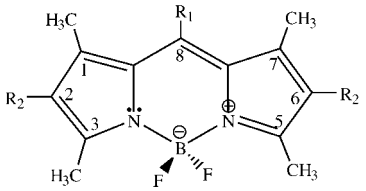


| Dye | $R_1$ | $R_2$ |
|---|---|---|
| PM650 | CN | $CH_3$ |
| PM546 | $CH_3$ | H |
| PM567 | $CH_3$ | $C_2H_5$ |
| PM597 | $CH_3$ | $t$-$C_4H_9$ |

***Figure 1.*** *General structure of pyrromethene dyes.*

mended for obtaining the highest lasing efficiency. However, the presence of high electron-donor or acceptor groups in the molecular structure can modify the photophysical properties of these dyes in such a way that it can enlarge the tunability range and/or improve their photostability and/or laser efficiency. In this regard, Jones et al.[31] recently reported drastic changes in the photophysical properties of PM dyes in the presence of a cyano group, and Rurack et al.[32–35] also reported an intramolecular charge-transfer state between an aniline group at the 8 position and the electronic $\pi$ system of the PM chromophore. In this system, the electronic excitation leads to an electron transfer from the aniline group to the aromatic ring. In apolar solvents emission occurs from the locally excited state (LE), but in polar solvents a high polar intramolecular charge-transfer state (ICT) is stabilised and populated from the LE state. The fluorescence from an ICT state is characterised by a large Stokes shift in polar solvents, which reduces the reabsorption/re-emission effects and the losses in the resonator cavity of tunable lasers. Moreover, due to the high sensibility of the photophysical properties of an ICT state to the nature of the solvent,[36–40] dyes that exhibit an ICT state are powerful tools as fluorescence molecular sensors in a multitude of systems, which include biological and chemical systems.[41–43]

In the present Article, the photophysics of the pyrromethene 650 (PM650) dye is studied. Besides the six methyl groups at the 1, 2, 3, 5, 6 and 7 positions, this dye has a high electron-acceptor cyano group at the symmetrical 8 position (Figure 1). The present results are compared with data previously obtained for other PM dyes, mainly with the results obtained for the well-known PM567[27] ($R_2$ = Ethyl in Figure 1). The photophysical properties of the PM650 dye are characterised in a wide variety of solvents (including apolar, polar and polar/protic media) and at several temperatures. The potential uses of this dye as active medium of tunable lasers and fluorescence probe are discussed from a photophysical point of view.

## Results and Discussion

UV/Vis absorption and fluorescence spectra and the radiative decay curves (analysed as a monoexponential decay) of PM650 in representative apolar and polar/protic solvents are depicted in Figure 2. The photophysical properties strongly change with respect to other PM dyes,[31] as can be seen in Table 1, where the absorption and fluorescence characteristics of PM650 are compared with the well-known PM567 derivative in an inert apolar solvent (cyclohexane).[27]

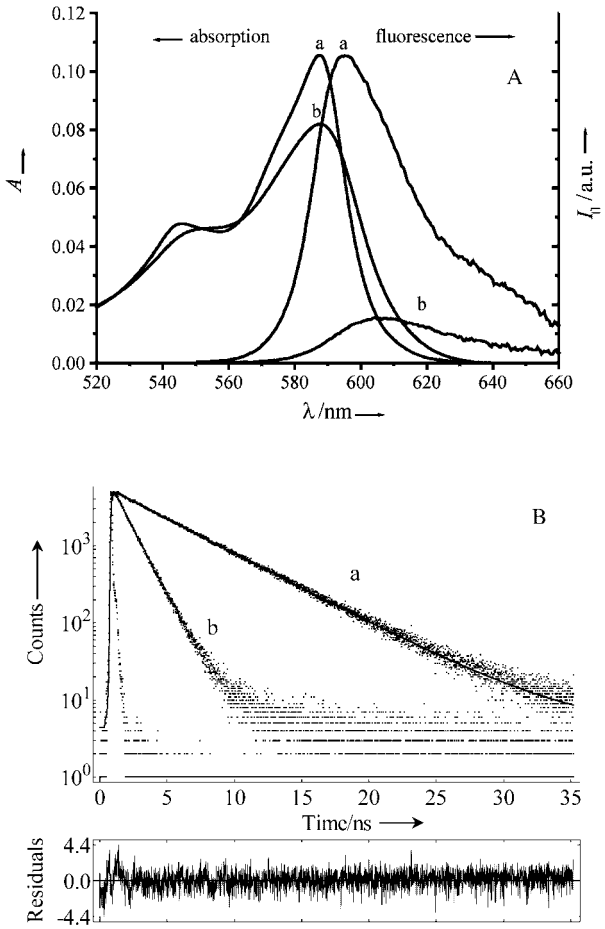


***Figure 2.*** *Absorption and corrected fluorescence spectra (A), and radiative decay curves (B) of diluted solutions ($2\times10^{-6}$ mol dm$^{-3}$) of PM650 in cyclohexane (a) and methanol (b). The residuals of the one-exponential decay in cyclohexane are also included ($\chi^2 = 1.14$).*

***Table 1.*** *Photophysical properties of diluted solutions ($2\times10^{-6}$ mol dm$^{-3}$) of PM650 and some alkyl-PM dyes (Figure 1) in cyclohexane at 20°C: absorption ($\lambda_{ab}$) and fluorescence ($\lambda_{fl}$) wavelengths, Stokes shift ($\Delta\nu_{St}$), molar absorption coefficient ($\varepsilon_{max}$), fluorescence quantum yield ($\phi$) and lifetime ($\tau$), and radiative ($k_{fl}$) and nonradiative ($k_{nr}$) deactivation rate constants. The photophysical characteristics of PM650 are specifically compared to those of PM567.*

| Dye | $\lambda_{ab}$ [±0.1 nm] | $\lambda_{fl}$ [±0.2 nm] | $\Delta\nu_{St}$ [cm$^{-1}$] | $\varepsilon_{max}$ [$10^4$ M$^{-1}$ cm$^{-1}$] | $\phi$ [±5%] | $\tau$ [ns, ±2%] | $k_{fl}$ [$10^8$ s$^{-1}$] | $k_{nr}$ [$10^8$ s$^{-1}$] |
|---|---|---|---|---|---|---|---|---|
| PM650 | 589.3 | 599.6 | 290 | 5.30 | 0.36 | 4.67 | 0.77 | 1.37 |
| PM546[14] | 499.4 | 509.6 | 400 | 9.74 | 0.77 | 5.23 | 1.47 | 0.45 |
| PM567[27] | 522.5 | 537.2 | 525 | 9.30 | 0.70 | 5.60 | 1.25 | 0.53 |
| PM597[30] | 529.0 | 571.2 | 1395 | 8.10 | 0.32 | 3.91 | 0.81 | 1.74 |
| comparison | $\Delta\nu_{ab}$ [cm$^{-1}$] | $\Delta\nu_{fl}$ [cm$^{-1}$] | $\Delta\nu_{St}$ [cm$^{-1}$] | $\varepsilon$ ratio | $\phi$ ratio | $\tau$ ratio | $k_{fl}$ ratio | $k_{nr}$ ratio |
| PM567-PM650 | 2170 | 1950 | 235 | 1.7 | 1.9 | 1.2 | 1.6 | 2.6 |

  

**Molecular Structure Effect**

The drastic shift to lower energies (around 2050 $cm^{-1}$) of the spectral bands of PM650 with respect to PM567, which is observed experimentally (Table 1), can be ascribed to the strong electron-acceptor capacity of the cyano group at the 8 position of the chromophore. In fact, alkyl substituents in any position of the PM chromophore do not produce such strong spectral shifts.[5,9,24] Quantum mechanics calculations also predict these relatively high spectral shifts. The absorption energy gap for the $S_0 \rightarrow S_1$ electronic transition can be estimated by the Franck–Condon transition from the geometry optimised in the ground $S_0$ state. Several calculation methods, at semiempirical and DFT levels, lead to similar optimised geometries of the ground $S_0$ state of PM650. Theoretical results reveal that the chromophore core of PM650 has a nearly planar structure with dihedral angles of about zero in the pyrrol units and in the six-folded ring that links the two pyrrol groups. Indeed, the B3LYP/6–31G calculation predicts, in the case of PM650, C-C1-C2-C3 and C1-C-C8-C (Figure 1) dihedral angles of 0.007° and 179.9°, respectively, which suggests a more planar $\pi$ aromatic ring than that observed for a PM567 dye (which has dihedral angles of 0.28° and 175.7°).

Because the presence of an electron-acceptor (or donor) substituent in the chromophoric $\pi$ system of PM dyes affects the charge distribution through the molecule, one would expect a higher Stokes shift in PM dyes with a cyano group than in those dyes with an alkyl group, that is, PM650 should show a higher shift than PM567. However, the opposite evolution in the $\Delta\nu_{St}$ value is experimentally observed (Table 1). This can be assigned to the position in which the cyano group is incorporated in the chromophoric system. Indeed, an electron-acceptor group at the central 8 position would create a negative charge density in such a way that it would partially neutralise the dipole moment of the PM chromophoric $\pi$ system oriented along the short molecular axis. This is confirmed by quantum mechanics calculations at the DFT level, in which the dipole moment in the ground state of PM650 (0.37 D) is predicted to be lower than that of PM567 (4.92 D).

The spectroscopic properties of the $S_0 \rightarrow S_1$ transition, calculated by time-dependent density-functional theory (TDDFT) and by the semiempirical "Zerner intermediate neglect of differential overlap" (ZINDO) and "configuration interaction singles and doubles" (CISD) methods, are summarised in Table 2. As can be deduced from the listed results, all theoretical methods overestimate the $S_0$–$S_1$ energy gap with respect to the experimental results. Actually, the most accurate TDDFT method provides the highest deviation; however, this method does predict the most realistic oscillator strength value (*f*), compared to the experimental one. The value of *f* is obtained from the area under the absorption band by means of Equation (1):[44]

***Table 2.*** *Absorption energy gap ($\Delta E_{ab}$, in eV) and oscillator strength (f) of PM650 calculated by TDDFT and the semiempirical ZINDO and CISD methods. The obtained data are compared with those of an inert solvent (cyclohexane, Table 1).*

| | PM650 | | PM567 | |
|---|---|---|---|---|
| | $\Delta E_{ab}$ [eV] | *f* | $\Delta E_{ab}$ [eV] | *f* |
| TDB3LYP/6–31G | 2.61 | 0.30 | 2.92 | 0.54 |
| ZINDO B3LYP/6–31G | 2.36 | 0.91 | 2.52 | 0.88 |
| ZINDO/AM1 | 2.36 | 0.94 | 2.50 | 0.89 |
| ZINDO/PM5 | 2.48 | 1.10 | 2.54 | 1.04 |
| CISD/AM1 | 2.46 | – | 2.57 | – |
| Experimental | 2.10 | 0.38 | 2.37 | 0.50 |

$$f = \frac{4.32 \times 10^{-9}}{n} \int \varepsilon(\nu) \mathrm{d}(\nu) \qquad (1)$$

where *n* is the refractive index of the solvent. Moreover, the experimentally observed diminution in the values of the energy gap and *f* for PM650 with respect to PM567 is better predicted by the TDDFT than by other semiempirical methods. These quantum mechanics calculations (Table 2) and the experimental results (Table 1) indicate that the presence of the cyano group reduces the energy gap and the probability of a spectroscopic transition between the $S_0$ and $S_1$ states.

Present quantum mechanics calculations confirm previous conclusions that the $S_0 \rightarrow S_1$ transition in pyrromethenes is mainly due to a promotion of one electron from the HOMO to the LUMO state.[42,45,46] The electronic density maps of these states for PM650 (Figure 3) suggest an important enhancement in the electron density at the central 8 position of the chromo-

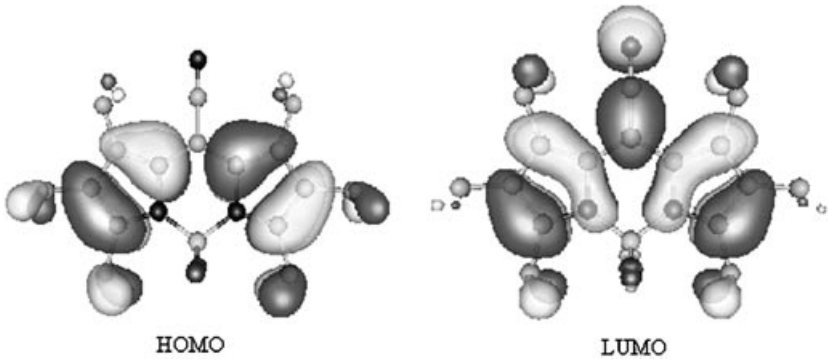


***Figure 3.*** *Electronic density maps for the HOMO and LUMO states of PM650 calculated by the semiempirical AM1 method.*

  

phore in the LUMO state with respect to the HOMO state. Thus, the presence of a high electron-withdrawing group, such as the cyano group, at this central position stabilises the LUMO state to a greater extent, causing a decrease in the LUMO–HOMO energy gap, which, of course, explains the bathochromic shift in both the absorption and the fluorescence bands of the PM650 dye with respect to PM567 (Table 1).

On the other hand, the molar absorption coefficient ($\varepsilon$) and the fluorescence rate constant ($k_{fl}$) decrease for PM650 with respect to PM567 (Table 1),[27] which is theoretically confirmed by the oscillator strength ($f$) (Table 2). The diminution of the radiative transition probability between $S_1$ and $S_0$ is attributed to a decrease in the electron density of the $\pi$ system of the chromophore, owing to the electron-acceptor character of the cyano group. This can be better analysed by the Mulliken or Coulson point charges obtained by DFT and semiempirical methods. The Mulliken charges on carbon atoms 8 and 1 (and on the symmetrical 7 position) for PM650 were calculated by the DFT method to be +0.195 and +0.153; these values are more positive than the corresponding 567 (i.e., +0.178 and +0.108, respectively). These differences are higher than those obtained by the semiempirical AM1 method, probably due to the tendency of the latter method to underestimate the electronegativity of the nitrogen atom. In any case, the present results indicate a reduction of the negative charge in the chromophore system, which is responsible for the observed decline in the radiative transition probability between the $S_0$ and $S_1$ states. Moreover, the fluorescence quantum yield of PM650 is also reduced (with respect to PM567) by an important augmentation (of a factor of about three in an apolar solvent such as cyclohexane, see Table 1) in the nonradiative deactivation process.

**Solvent Effects: Absorption and Fluorescence Bands**

To gain a deeper knowledge of the influence of the cyano group on the photophysical properties of PM650, the solvent effect on the photophysical characteristics of this dye was recorded. The important influence of the medium on the fluorescence properties of the dye is illustrated in Figure 2, where a drastic decrease in the fluorescence intensity and the lifetime in a polar/protic environment (methanol) with respect to an apolar, inert solvent (cyclohexane) can be observed. The photophysical properties of PM650 in several apolar, polar and protic solvents are summarised in Table 3. It is worth noting that the absorption and fluorescence spectra of the dye were found to be time-dependent in several electron-donor solvents (such as dimethylformamide, dimethylacetamide, 2-pentanone, etc). This observation was also detected for samples aged in the dark. Depending on the nature of the environment, an important decline in both spectral intensities of PM650 was observed after several hours or a few days. In some cases, the bleaching or a change in the global colour of the sample was induced. Further research is currently being carried out in our laboratory to explain the chemical nature of this phenomenon.

From the results shown in Table 3 it is difficult to establish a clear dependence of the position of the absorption band with the nature of the solvent, although a slight bathochromic shift (not longer than 4 nm) could be estimated from apolar to polar/protic solvents. These results suggest that several solvent parameters may induce different spectral shifts in the absorption band, as will be discussed later. In any case, an important change in the dipole moment between the $S_0$ and the $S_1$ Franck–Condon states during the absorption process can be discarded, since the absorption band does not show a clear shift with the solvent polarity.

***Table 3.*** *Photophysical properties of diluted solutions ($2\times10^{-6}$ mol dm$^{-3}$) of PM650 in several solvents at room temperature.*

| Solvent | $\lambda_{ab}$ [±0.1 nm] | $\varepsilon_{max}$ [$10^4$ M$^{-1}$ cm$^{-1}$] | $\lambda_{fl}$ [±0.2 nm] | $\Delta\nu_{St}$ [cm$^{-1}$] | $\phi$ [±5%] | $\tau$ [ns, ±2%] | $k_{nr}$ [$10^8$ s$^{-1}$] |
|---|---|---|---|---|---|---|---|
| 1. 2-methylbutane | 586.6 | 5.28 | 596.0 | 270 | 0.45 | 5.23 | 1.05 |
| 2. n-hexane | 587.6 | 5.20 | 597.2 | 275 | 0.44 | 5.14 | 1.09 |
| 3. cyclohexane | 589.3 | 5.30 | 599.6 | 290 | 0.36 | 4.67 | 1.37 |
| 4. isooctane | 587.5 | 5.28 | 597.2 | 275 | 0.41 | 4.86 | 1.21 |
| 5. diethyl ether | 587.4 | 3.65 | 601.6 | 400 | 0.30 | 3.44 | 2.04 |
| 6. 1,4-dioxane | 589.8 | 4.25 | 607.2 | 485 | 0.19 | 2.89 | 2.80 |
| 7. tetrahydrofurane | 590.0 | 2.93 | 606.4 | 460 | 0.18 | 2.46 | 3.33 |
| 8. acetone | 587.9 | 3.45 | 606.0 | 510 | 0.11 | 1.81 | 4.92 |
| 9. methyl formate | 587.6 | 4.25 | 605.2 | 495 | 0.15 | 2.17 | 3.92 |
| 10. methyl acetate | 587.8 | 4.25 | 604.8 | 480 | 0.16 | 2.38 | 3.53 |
| 11. ethyl acetate | 587.8 | 4.17 | 603.2 | 435 | 0.15 | 2.37 | 3.59 |
| 12. buthyl acetate | 588.9 | 4.48 | 603.6 | 415 | 0.19 | 2.71 | 2.99 |
| 13. acetonitrile | 588.0 | 2.85 | 605.6 | 495 | 0.096 | 1.73 | 5.23 |
| 14. 1-octanol | 591.1 | 4.37 | 605.6 | 405 | 0.17 | 2.58 | 3.22 |
| 15. 1-hexanol | 590.5 | 4.29 | 607.6 | 475 | 0.14 | 2.31 | 3.72 |
| 16. 1-butanol | 590.0 | 4.17 | 607.6 | 490 | 0.13 | 2.02 | 4.30 |
| 17. 1-propanol | 589.6 | 4.00 | 606.8 | 480 | 0.13 | 1.83 | 4.75 |
| 18. ethanol | 588.7 | 4.05 | 608.0 | 540 | 0.099 | 1.64 | 5.49 |
| 19. methanol | 587.5 | 4.10 | 609.2 | 606 | 0.060 | 1.29 | 7.29 |
| 20. trifluoroethanol | 589.9 | 3.80 | 614.4 | 675 | 0.040 | 1.14 | 8.42 |

  

However, the fluorescence band clearly shifts to lower energies (around 15 nm) from an apolar to a polar/protic environment (Table 3), which leads to a significant increase in the Stokes shift in polar solvents. These results suggest an important increase in the dipole moment of the relaxed $S_1$ excited state of the molecule during its lifetime.

The solvent effect on the fluorescence wavenumber ($\nu_{fl}$) and the Stokes shift ($\Delta\nu_{St}$) is described on the basis of a multilinear regression analysis (in which several physicochemical properties of the solvent are simultaneously considered) by means of Equation (2):

$$(XYZ) = (XYZ)_0 + c_aA + c_bB + c_cC + \ldots \quad (2)$$

where $(XYZ)_0$ is the physicochemical property of interest in an inert solvent and $c_a$, $c_b$, $c_c$,... are the adjusted coefficients that reflect the dependency of the physicochemical property (*XYZ*) with different *A, B, C*,... solvent parameters. In the present analysis, the solvent polarity/polarisability and the H-bond and electron-donor capacities of the solvent are taken into account. At least two different set scales can be found in the literature to characterise these solvent properties: Taft et al.[47] proposed the $\pi^*$, $\alpha$ and $\beta$ scales to characterise, respectively, the polarity/polarisability, the acidity and the basicity of the solvent; whereas Catalán et al.[48] suggested the $SPP^N$, the SA and the SB scales to characterise the above-mentioned properties of a solvent. Figure 4 shows a satisfactory linear correlation (correlation coefficient $r > 0.95$) between the experimental $\nu_{fl}$ and $\Delta\nu_{St}$ values and the corresponding expected values obtained by the multicomponent regression using the Taft solvent scale. Table 4 lists the adjusted coefficients of several solvent parameters for $\nu_{ab}$, $\nu_{fl}$ and $\Delta\nu_{St}$ values of PM650, as well as the correlation coefficients obtained with both the Taft and the Catalán solvent scales. Both sets of parameters induce similar qualitative results, although the Taft scale provides better correlation coefficients (*r*) and more accuracy in the adjusted coefficients for the PM650 dye studied in this work. Previous results for other PM dyes suggested more accurate adjustments with the Catalán scale than with the Taft scale.[14,15,27] Therefore, the Taft parameters seem to be a better approach when an electron-transfer process affects the physicochemical properties under study.

***Table 4.*** *Multilinear regression analysis of the absorption ($\nu_{ab}$), fluorescence ($\nu_{fl}$) and Stoke shift ($\Delta\nu_{St}$) wavenumber of PM650 dye, with several solvent parameters described by the Taft scales[47] (polarity/polarisability, $\pi^*$, H-bond donor capacity, $\alpha$, and electron-donor ability, $\beta$) and by the Catalán scales[48] (polarity/polarisability, $SPP^N$, acidity, SA, and basicity, SB).*

| Taft scale | $(\nu_\infty)_0$ [$cm^{-1}$, ±10] | $c_{\pi^*}$ [±30] | $c_\alpha$ [±15] | $c_\beta$ [±25] | *r* |
|---|---|---|---|---|---|
| $\nu_{ab}$ | 17010 | – | 30 | 40 | 0.58 |
| $\nu_{fl}$ | 16720 | −325 | −125 | – | 0.96 |
| $\Delta\nu_{St}$ | 290 | 330 | 100 | −45 | 0.97 |
| **Catalán scale** | $(\nu_\infty)_0$ [$cm^{-1}$, ±60] | $c_{SPP^N}$ [±100] | $c_{SA}$ [±40] | $c_{SB}$ [±40] | *r* |
| $\nu_{ab}$ | 17000 | – | 45 | 75 | 0.63 |
| $\nu_{fl}$ | 17064 | −650 | −175 | – | 0.95 |
| $\Delta\nu_{St}$ | −60 | 680 | 130 | −70 | 0.95 |

Both solvent scales suggest that the solvent polarity/polarisability is the main solvent parameter responsible for the shift of the fluorescence band to lower energies (high and positive $c_{\pi^*}$ and $c_{SPP^N}$ values, Table 4). The fluorescence band is also influenced by the solvent acidity (H-bond capacity). The basicity of the environment (electron-donor ability) does, on the other hand, not affect the fluorescence band position (nearly negligible $c_\beta$ and $c_{SB}$ values, Table 4). The slight decrease in the Stokes shift with the solvent basicity is due to a low bathochromic shift observed in the absorption band, which is partially compensated by the solvent acidity.

The present multilinear analysis suggests that, contrary to the behaviour observed for other commercial PM dyes,[14,15,27] the relaxed excited state of PM650 is more polar than the ground state. Since the electron transfer process is favoured in the excited state, a redistribution of the electronic $\pi$ system of the PM chromophore takes place during the lifetime of the $S_1$ excited state, and a net electronic charge can be transferred to the cyano group. This electron redistribution augments the dipole moment of the chromophore along the short molecular axis. As a consequence, the $S_1$ state is more stable in polar solvents. This can be extended to acidic media, since H-bond donor solvents partly neutralise the negative charge localised at the cyano group.

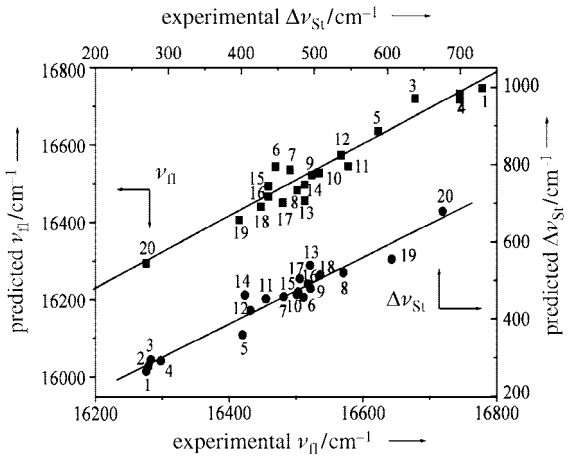


***Figure 4.*** *Linear correlation between the experimental and predicted values of the fluorescence ($\nu_{fl}$, ■) and Stokes-shift ($\Delta\nu_{St}$, ●) wavenumber obtained by means of a multilinear regression analysis in which the Taft[47] solvent polarity/polarisability ($c_{\pi^*}$), acidity ($c_\alpha$) and basicity ($c_\beta$) are simultaneously analysed. The solvent numbers are listed in Table 2.*

  

Contrary to the well-defined fluorescence band shift, the unclear evolution of the absorption wavelength mentioned above is reflected by its low correlation coefficients (Table 4) and the misleading behaviour of the solvent acidity and basicity. Solvent polarity has a negligible effect on the absorption band position due to the low dipole moment of PM650. As is mentioned above, the ground state of PM650 is characterised by a low dipole moment ($<1$ D, depending on the calculation method), lower than that of other alkyl derivatives ($\approx 4.5$ D for PM567). This diminution in PM650 is a consequence of the presence of the strong electron-withdrawing cyano group at position 8, which destabilises the electronic density at this position.

The charge distribution can be qualitatively analysed by the resonance structures of the chromophore shown in Figure 5. Thus, the resonance structure "a" (Figure 5), with the highest charge separation along the short molecular axis, has a lower statistical weight in PM650 than in other PM dyes, which explains the low dipole moment in the ground state of the former dye. This is qualitatively confirmed by the bond length alternation (BLA) parameter obtained from theoretical calculations,[49] which can be considered as a value for the delocalisation in aromatic $\pi$ systems. A higher BLA value is ascribed to a lower statistical weight of the more delocalised resonance structure, that is, the resonance structure "a" (Figure 5) for PM dyes. The BLA value of PM650 (0.027) is higher than that of PM567 (0.022), which supports the presence of a low dipole moment (less statistical weight of resonance structure "a") in the former dye.

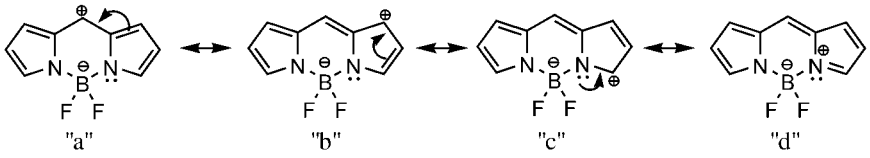


***Figure 5.*** *Resonance structures of the PM chromophore.*

Theoretical calculations suggest an increase ($\Delta\mu \approx 1$ D) in the dipole moment of PM650 in the Franck–Condon excited state with respect to the ground state; this is the opposite behaviour to that observed in other commercial alkyl PMs, where the excitation leads to a diminution in the dipole moment. This difference is attributed to an enhancement in the electron-withdrawing effect of the cyano group after excitation of the electronic $\pi$ system of PM650, which increases the localisation of the negative charge on the cyano group. This effect leads to an inversion in the orientation of the dipole moment through the short molecular axis upon excitation, which is not reflected in an important modification of the absolute value of the dipole moment. In PM567, the inductive effect $+I$ of the ethyl group increases the dipole moment of the $\pi$ system upon excitation.

**Solvent Effects: Radiative and Nonradiative Deactivation Rate Constants**

The influence of the medium is most significant on the fluorescence quantum yield ($\phi$) and on the lifetime ($\tau$) of PM650, with an important decline in polar/protic solvents (Table 3), which suggests an important quenching process in these environments. The rate constants of radiative ($k_{fl}$) and nonradiative ($k_{nr}$) processes show a relatively good linear relationship (in a logarithmic scale) with the solvent polarity and acidity described by the Reichardt $E_T^N(30)$ solvent parameter (Figure 6A).[50] However, some deviations from this linearity can be observed in low-polar media for a series of common solvents, for instance, in hydrocarbons [2-methyl butane (1), n-hexane (2), cyclohexane (3) and isooctane (4)], and in alcohols [1-octanol (14), 1-hexanol (15) and 1-butanol (16)]. In Figure 6B the solvent effect on the $k_{nr}$ value is analysed in terms of the multilinear regression method, which improves the correlation coefficient ($r = 0.97$) against the $E_T^N(30)$ representation ($r = 0.84$). The multicomponent analysis suggests that the $k_{nr}$ value of PM650 increases with the solvent polarity/polarisability ($c_{\pi^*} \approx 5.3 \times 10^8\ s^{-1}$) and with the H-bond donor capacity ($c_\alpha \approx 2.5 \times 10^8\ s^{-1}$), but diminishes with the electron-releasing capacity of the solvent ($c_\beta \approx -1.5 \times 10^8\ s^{-1}$).

The enhancement of the dipole moment of the $S_1$ relaxed state with respect to the $S_0$ state is not incompatible with the decrease of the radiative transition dipole moment (analysed by the parameters $k_{fl}$ and $\varepsilon$ in Table 1)[44] between both states in polar/protic solvents. Indeed, the dipole moment is along the short molecular axis, whereas the $S_1 \rightarrow S_0$ spectral transition is polarised through the long molecular axis, as theoretical calculations suggest.[42,45,46]

**Deactivation via an Intramolecular Charge-Transfer (ICT) State**

Several experimental observations discussed above suggest the formation of an intramolecular charge-transfer (ICT) state from the excited state of PM650.[32,36] Such observations are, for example, the important increase in the $k_{nr}$ value in polar media (Table 3) and the better correlation of the $k_{nr}$ value with the multilinear regression (Figure 6B) than with the $E_T^N(30)$ parameter (Figure 6A). The ICT state should be formed by the transfer of one electron from the electronic $\pi$ system of the PM chromophore to the cyano group, and it could induce a new nonradiative deactivation from the local excited state, as is illustrated in Scheme 1. A similar but inverse electron transfer for an electron-donor substituent (aniline) to the electronic $\pi$ system of a PM chromophore was previously reported by Rurack et al.[32–35] for the observed declination of the fluorescence intensity of the corresponding PM derivative. The ICT state of PM650 should not be fluorescent under the experi-

  

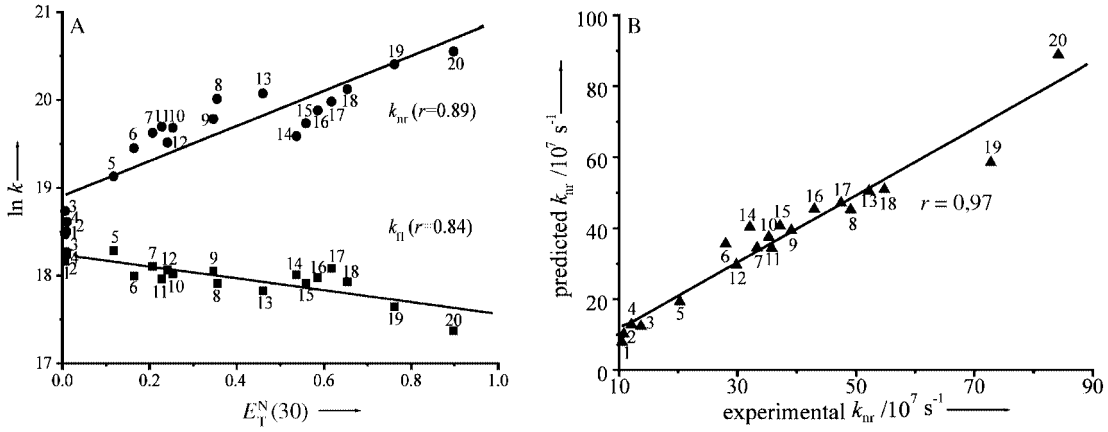


***Figure 6.*** *A) Radiative ($k_{fl}$ ■) and nonradiative ($k_{nr}$ ●) deactivation rate constants of PM650 correlated with the Reichardt solvent parameter $E_T^N(30)$.[50] B) Linear correlation between the experimental $k_{nr}$ and predicted values obtained by means of the multilinear regression analysis described in the caption of Figure 4. The solvent numbers are listed in Table 2.*

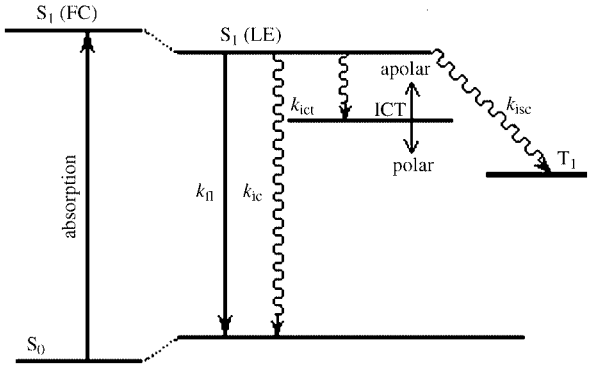


***Scheme 1.*** *Energy diagram for the deactivation processes from the $S_1$ excited state of PM650: LE (localised excited), FC (Franck–Condon) and ICT (intramolecular charge-transfer) states. Continuous and wavy lines represent radiative and nonradiative processes, respectively. The stabilisation of the ICT state with the solvent polarity is also illustrated.*

mental conditions used in this work, since an additional emission band at lower energies with respect to the $S_1$ fluorescence band was not experimentally observed in polar/protic solvents. The corresponding rate constant ($k_{ict}$) should be solvent-dependent, since the stabilisation of the ICT state is strongly favoured in polar media (Scheme 1).[36–40] Taking into account that the fluorescence decay curve of PM650 is analysed as a one-exponential decay in all considered solvents, the reversible process of an electron transfer from the ICT state to the localised $S_1$ excited state should be negligible.

The $k_{nr}$ value of PM650 (Table 3) includes the rate constants of internal conversion ($k_{ic}$), intersystem crossing ($k_{isc}$) and ICT-state formation ($k_{ict}$). The $k_{isc}$ value of commercial PM dyes is very low and an extra enhancement in this process by the presence of the cyano group should not be expected.[21–24] Previous works on several alkyl- and aromatic-substituted PM dyes have associated the $k_{ic}$ value with the rigidity of the aromatic PM ring (this rigidity being identified with the planarity of the aromatic system).[15,29,30,51] Indeed, bulky *t*-butyl groups at positions 2 and 6, or a phenyl ring at position 8, of the PM chromophore augment the internal conversion of the PM dye, due to a disruption in the planarity of the pyrrol rings, or in that of the six-folded ring that links the pyrrol rings, which is caused by steric hindrances with adjacent methyl groups.[30,51] Considering that the calculated geometry of PM650 suggests a planar aromatic core, a similar $k_{ic}$ value is expected for PM650 as for other commercial PM dyes without any bulky substituents directly attached to the PM core, such as PM546 and PM567 (Figure 1). Consequently, the solvent dependency of the $k_{nr}$ values of PM650 should be mainly ascribed to environmental effects on the intramolecular charge-transfer process. Indeed, the ICT state should be characterised by a high dipole moment, and a stabilisation of this state in polar solvents would enhance the corresponding rate constant.

To know more about the dynamics of the ICT formation, the photophysical properties of PM650 were recorded as a function of the temperature in apolar (cyclohexane) and polar (ethanol) solvents (Table 5). The decrease in the $\phi$ and $\tau$ values with increasing temperature is due to an augmentation of the nonradiative processes at high temperatures, rather than to a

***Table 5.*** *Fluorescence quantum yield ($\phi$) and lifetime ($\tau$), and rate constant of the nonradiative deactivation ($k_{nr}$) of PM650 in cyclohexane and ethanol at different temperatures. The $\phi$ values are corrected from the variation of the refractive index of the solvent with the temperature.*

| $T$ [K] | cyclohexane | | | ethanol | | |
|---|---|---|---|---|---|---|
| | $\phi$ [±5%] | $\tau$ [ns, ±2%] | $k_{nr}$ [10$^8$ s$^{-1}$] | $\phi$ [±5%] | $\tau$ [ns, ±2%] | $k_{nr}$ [10$^8$ s$^{-1}$] |
| 293 | 0.38 | 4.82 | 1.29 | 0.104 | 1.74 | 5.15 |
| 303 | 0.36 | 4.62 | 1.39 | 0.098 | 1.62 | 5.56 |
| 313 | 0.34 | 4.49 | 1.47 | 0.092 | 1.52 | 5.97 |
| 323 | 0.33 | 4.35 | 1.54 | 0.085 | 1.43 | 6.39 |
| 333 | 0.31 | 4.13 | 1.67 | 0.080 | 1.35 | 6.81 |

  

diminution of the radiative deactivation (which is observed to be nearly temperature-independent). The values of $k_{nr}$ follow the Arrhenius behaviour ($r > 0.99$) with an activation energy ($E_a$) of about 5.4 kJ mol$^{-1}$ in both solvents. This is not the case for PM567 where an $E_a$ value of 2.1 kJ mol$^{-1}$ (in cyclohexane) and 5.4 kJ mol$^{-1}$ (in methanol) can be derived from the $\phi$ and $\tau$ values previously published.[27] If, for a common solvent, both PM dyes have similar internal conversion processes, and considering that the nonradiative deactivation via the ICT state is only possible in the PM650 dye, these results suggest that the activation energy for the ICT formation in the $S_1$ excited state is almost negligible in the polar/protic environment, whereas the formation of the ICT state in an apolar solvent (cyclohexane) would have an energy barrier (of about 3.3 kJ mol$^{-1}$) associated to it. These results are consistent with the stabilisation of the ICT state in polar solvents (Scheme 1), which reduces the activation energy for the electron-transfer process.

From a photophysical point of view, apolar media are recommended to achieve the highest laser efficiency of PM650 in liquid solutions, since the highest fluorescence quantum yields are obtained in these kinds of solvent. This contrasts with preceding conclusions obtained for other commercial PM dyes (PM546 and PM567),[14,27] where the highest $\phi$ values and laser efficiencies were observed in polar solvents. Due to the lower $\phi$ value of PM650 with respect to PM567,[27] one should not expect such a high laser efficiency in the former dye. However, due to the important shift in the fluorescence band of PM650, this dye enlarges the tunability range of PM dyes from the green–yellow spectral region to the red.

On the other hand, PM650 presents a higher resistance to oxygen attack than other commercial PM dyes.[31] This recent observation would improve the photostability of this dye, since PM dyes are sensitive to reactions with oxygen due to the presence of amine aromatic groups.[26,52]

Finally, and owing to the important dependence of the photophysical properties of PM650 on the nature of the solvent, this dye is an adequate candidate to be used as fluorescent probe in systems of interest, such as biological and micro-heterogeneous systems, monolayers, films and nanostructured systems.[41–43]

Summarising, the photophysical properties of the PM650 dye are different to those of other commercial pyrromethene dyes. The strong bathochromic shift observed in both absorption and fluorescence bands is assigned to the high electron-acceptor character of the cyano group present at the 8 position of the PM650 chromophore. This group induces a new nonradiative deactivation process for the PM chromophore, via an intramolecular charge-transfer ICT state, as a consequence of the electron transfer from the electronic $\pi$ system of the chromophore to the cyano group during the lifetime of the locally excited state. The ICT state is formed even in apolar environments with a low activation energy (of around 3 kJ mol$^{-1}$). The ICT state is favoured in polar/protic solvents, owing to the high dipole moment that characterises this state, without any appreciable energy barrier. This extra deactivation process decreases the fluorescent efficiency of the PM650 dye and, for this reason, apolar environments are recommended for this dye as active media in tunable lasers. Because of the low fluorescence quantum yield, PM650 is expected to have a lower laser efficiency than other commercial PM dyes, although the former dye improves the operating lifetime of the active media of tunable lasers due to its higher photostability.[31] The strong dependence of the fluorescence properties of the PM650 dye on the nature of the solvent should increase the tunability range of the laser signals of PM dyes and enhance the applicability of these dyes as fluorescent probes for studying a multitude of interesting chemical and biological systems.

## Experimental Section and Computational Methods

Pyrromethene 650, PM650, (1, 2, 3, 5, 6, 7-hexamethyl-8-cyanopyrromethene-$BF_2$) dye (Exciton, laser grade) and all the solvents (Merck, Sigma or Aldrich, spectroscopic grade) were used without further purification. Diluted dye solutions ($2\times10^{-6}$ mol dm$^{-3}$) were prepared by dissolving the appropriate amount of the dye (obtained from a concentrated stock solution, $10^{-3}$ mol dm$^{-3}$, of the dye) in acetone after solvent vacuum evaporation. The photophysical properties were recorded immediately after sample preparation.

Instrumental: Absorption and fluorescence spectra (after excitation at $\lambda \approx 540$ nm) were recorded on a Cary 4E spectrophotometer and a Shimadzu spectrofluorimeter (RF-5000 model), respectively, with 1 cm quartz cuvettes. The fluorescence spectra were corrected for the wavelength dependence of the monochromator and the photomultiplier sensitivity. The fluorescence quantum yield ($\phi$) was evaluated using a diluted solution of PM567 in methanol ($\phi = 0.91$ at 20 °C)[27] as the reference and was corrected from the dependence of the refractive index of the solvent.
Radiative decay curves were recorded by the time-correlated single-photon counting technique (Edinburgh Instruments model ηF900). The emission was monitored at about $\lambda \approx 585$ nm after excitation ($\lambda \approx 540$ nm) by means of a hydrogen flashlamp with a width-at-middle-height of 1.5 ns pulses and a 40 kHz repetition rate. The instrument was equipped with a red-sensitive photomultiplier (Hamamatsu R955). Fluorescence decay curves were analysed as a one-exponential decay ($\chi^2 < 1.2$ ) and the fluorescence decay time ($\tau$) was obtained from the slope. The estimated errors in the determination of $\phi$ and $\tau$ values are 5% and 2%, respectively. The rate constants for the radiative ($k_{fl}$) and nonradiative ($k_{nr}$) deactivation processes were calculated by: $k_{fl} = \phi/\tau$ and $k_{nr} = (1-\phi)/\tau$. The measurements were carried out on aerated samples. The temperature of the samples was controlled by an external flow of thermostated water.

Computational: Theoretical calculations were performed at the DFT,[53] (B3LYP)[54,55] and semiempirical AM1[56] and PM5 levels. Several commercial softwares (Gaussian 98,[57] MOPAC 2002[58] included in CAChe 5.0) were used. The optimisation of the geometry in the ground state by the DFT method was carried out using the 6–31G and 6–31G* basis sets and the default options for convergence. For semiempirical calculations, the minimum gradient for convergence was imposed at 0.01 kcal mol$^{-1}$ Å$^{-1}$ (precise) and the eigenvector following routine was used.[59] In both cases, no geometrical restrictions were imposed during the optimisation procedure, and the geometry was considered to be optimised when the corresponding frequency analysis did not give any negative value.
The absorption characteristics were simulated by the time-dependent DFT (TDB3LYP, in Gaussian 98)[60] method, the semiempirical

  

Zerner's intermediate neglect of differential overlap (ZINDO,[61] in Gaussian 98 and MOPAC 2002) method and the semiempirical configuration interaction singles and doubles method (CISD, with 361 configurations in MOPAC 2002). These calculation methods were applied to the optimised geometry of PM650 obtained by the DFT and semiempirical calculations mentioned above.

## Acknowledgements

*This work was supported by the Spanish MCyT Minister (MAT2000–1361-C04–02) and the Basque County University UPV/EHU (9/UPV00039.310–15264/2003). J.B.P. and V.M.M. thank the UPV/EHU and the MECD Minister for research grants.*

**Keywords:** charge transfer · photophysics · pyrromethene dyes · quantum mechanics calculations · solvent effects

[1] F. J. Duarte, *Tunable Lasers Handbook*, Academic Press, San Diego, California, **1995**.
[2] M. Maeda, *Laser Dyes*, Academic Press, London, **1984**.
[3] F. J. Duarte, *Tunable Lasers Applications*, Academic Press, New York, **1995**.
[4] K. H. Drexhage, *Dye Lasers*, (Ed.: F. P. Schäfer), Springer-Verlag, Berlin, **1990**, pp. 156 – 200.
[5] M. D. Rahn, T. A. King, *Appl. Opt.* **1995**, *34*, 8260 – 8271.
[6] E. Yariv, S. Schultheiss, T. Saraidarov, R. Reisfeld, *Opt. Mater.* **2001**, *16*, 29 – 38.
[7] A. Costela, I. García-Moreno, C. Gómez, O. García, R. Sastre, *Chem. Phys. Lett.* **2003**, *369*, 656 – 661.
[8] A. Costela, I. García-Moreno, R. Sastre, *Phys. Chem. Chem. Phys.* **2003**, *5*, 4745 – 4763.
[9] Y. Yang, M. Wang, G. Qian, Z. Wang, X. Fan, *Opt. Mater.* **2004**, *24*, 621 – 628.
[10] M. Shah, K. Thangaraj, M-L. Soong, L. T. Wolford, J. H. Boyer, I. R. Politzer, T. G. Pavlopoulos, *Heteroat. Chem.* **1990**, *1*, 389 – 399.
[11] J. H. Boyer, A. M. Haag, G. Sathyamoorthi, M-L. Soong, K. Thangaraj, T. G. Pavlopoulos, *Heteroat. Chem.* **1993**, *4*, 39 – 48.
[12] J. Karolin, L. B-A. Johansson, L. Strandberg, T. Ny, *J. Am. Chem. Soc.* **1994**, *116*, 7801 – 7806.
[13] F. Li, S. I. Yang, T. Ciringh, J. Seth, C. H. Martin III, D. L. Singh, D. Kim, R. R. Birge, D. F. Bocian, D. Holten, J. S. Lindsey, *J. Am. Chem. Soc.* **1998**, *120*, 10001 – 10017.
[14] F. López Arbeloa, T. López Arbeloa, I. López Arbeloa, *J. Photochem. Photobiol. A* **1999**, *121*, 177 – 182.
[15] F. López Arbeloa, T. López Arbeloa, I. López Arbeloa, *Recent Res. Devel. Photochem. Photobiol.* **1999**, *3*, 35 – 49.
[16] P. Toele, H. Zhang, C. Trieflinger, J. Daub, *Chem. Phys. Lett.* **2003**, 368, 66 – 75.
[17] T. G. Pavlopoulos, M. Shah, J. H. Boyer, *Appl. Opt.* **1988**, *27*, 4998 – 4999.
[18] T. G. Pavlopoulos, M. Shah, J. H. Boyer, *Opt. Commun.* **1989**, *70*, 425 – 427.
[19] J. H. Boyer, A. Haag, M-L. Soong, H. Thangaraj, T. G. Pavlopoulos, *Appl. Opt.* **1991**, *30*, 3788 – 3789.
[20] M. P. O'Neil, *Opt. Lett.* **1993**, *18*, 37 – 38.
[21] T. G. Pavlopoulos, *Appl. Opt.* **1997**, *36*, 4969 – 4980.
[22] A. A. Gorman, I. Hamblett, T. A. King, M. D. Rahn, *J. Photochem. Photobiol. A* **2000**, *130*, 127 – 132.
[23] F. Liang, H. Zeng, Z. Sun, Y. Yuan, Z. Yao, Z. Xu, *J. Opt. Soc. Am. B.* **2001**, *18*, 1841 – 1845.
[24] T. G. Pavlopoulos, *Prog. Quantum Electron.* **2002**, *26*, 193 – 224.
[25] M. S. Mackey, W. D. Sisk, *Dyes Pigm.* **2001**, *51*, 79 – 85.
[26] M. D. Rahn, T. A. King, A. A. Gorman, I. Hamblett, *Appl. Opt.* **1997**, *36*, 5862 – 5871.
[27] F. López Arbeloa, T. López Arbeloa, I. López Arbeloa, I. García-Moreno, A. Costela, R. Sastre, F. Amat-Guerri, *Chem. Phys.* **1998**, *236*, 331 – 341.
[28] T. López Arbeloa, F. López Arbeloa, I. López Arbeloa, I. García-Moreno, A. Costela, R. Sastre, F. Amat-Guerri, *Chem. Phys. Lett.* **1999**, *299*, 315 – 321.
[29] A. Costela, I. García-Moreno, C. Gómez, R. Sastre, F. Amat-Guerri, M. Liras, F. López Arbeloa, J. Bañuelos Prieto, I. López Arbeloa, *J. Phys. Chem. A.* **2002**, *106*, 7736 – 7742.
[30] J. Bañuelos Prieto, F. López Arbeloa, V. Martínez Martínez, T. Arbeloa López, I. López Arbeloa, *J. Phys. Chem. A* **2004**, *108*, 5503 – 5508.
[31] G. Jones II, S. Kumar, O. Klueva, D. Pacheco, *J. Phys. Chem. A.* **2003**, *107*, 8429 – 8434.
[32] M. Kollmannsberger, R. Rurack, U. Resch-Genger, W. Rettig, J. Daub, *Chem. Phys. Lett.* **2000**, *329*, 363 – 369.
[33] M. Kollmannsberger, T. Gareis, S. Heinl, J. Breu, J. Daub, *Angew. Chem.* **1997**, *109*, 1391 – 1393; M. Kollmannsberger, T. Gareis, S. Heinl, J. Breu, J. Daub, *Angew. Chem. Int. Ed. Engl.* **1997**, *36*, 1333 – 1335.
[34] M. Kollmannsberger, K. Rurack, U. Resch-Genger, J. Daub, *J. Phys. Chem. A.* **1998**, *102*, 10211 – 10220.
[35] K. Rurack, M. Kollmannsberger, U. Resch-Genger, J. Daub, *J. Am. Chem. Soc.* **2000**, *122*, 968 – 969.
[36] N. Chattopadhyay, C. Serpa, M. M. Pereira, J. Seixas de Melo, L. G. Arnaut, S. J. Formosinho, *J. Phys. Chem. A.* **2001**, *105*, 10025 – 10030.
[37] A. Onkelinx, F. C. De Schryver, L. Viaene, M. Van der Auweraer, K. Iwai, M. Yamamoto, M. Ichikawa, H. Masuhara, M. Maus, W. Rettig, *J. Am. Chem. Soc.* **1996**, *118*, 2892 – 2902.
[38] A. L. Sobolewski, W. Sudholt, W. Domcke, *J. Phys. Chem. A.* **1998**, *102*, 2716 – 2722.
[39] A. B. L. Parusel, W. Rettig, K. Rotkiewicz, *J. Phys. Chem. A.* **2002**, *106*, 2293 – 2299.
[40] S. Zilberg, Y. Haas, *J. Phys. Chem. A.* **2002**, *106*, 1 – 11.
[41] Y-P. Yang, C-T. Kuo, C-S. Yan, K-C. Lin, W-C. Huang, T-C. Chang, *Phys. Chem. Chem. Phys.* **2000**, *2*, 5271 – 5274.
[42] F. Bergström, I. Mikhailov, P. Hägglof, R. Wortmann, T. Ny, L.B-A. Johansson, *J. Am. Chem. Soc.* **2002**, *124*, 196 – 204.
[43] V. Buschmann, K. D. Weston, M. Sauer, *Bioconjugate Chem.* **2003**, *14*, 195 – 204.
[44] J. B. Birks, *Photophysics of Aromatic Molecules*, Wiley Interscience, London, **1970**.
[45] a) J. Bañuelos Prieto, F. López Arbeloa, V. Martínez Martínez, I. López Arbeloa, *Chem. Phys.* **2004**, *296*, 13 – 22; b) J. Bañuelos Prieto, F. López Arbeloa, V. Martínez Martínez, T. Arbeloa López, I. López Arbeloa, *Phys. Chem. Chem. Phys.* **2004**, *6*, 4247 – 4253.
[46] P. Acebal, S. Blaya, L. Carretero, *Chem. Phys. Lett.* **2003**, *374*, 206 – 214.
[47] a) M. J. Kamlet, R. W. Taft, *J. Am. Chem. Soc.* **1976**, *98*, 377 – 383; b) R. W. Taft, M. J. Kamlet, *J. Am. Chem. Soc.* **1976**, *98*, 2886 – 2894; c) M. J. Kamlet, J. L. M. Abboud, R. W. Taft, *J. Am. Chem. Soc.* **1977**, *99*, 6027 – 6038.
[48] a) J. Catalán, V. López, P. Pérez, *J. Fluorescence* **1996**, *6*, 15 – 21; b) J. Catalán, J. Palomar, C. Díaz, J. L. Paz, *J. Phys. Chem.* **1997**, *101*, 5183 – 5189; c) J. Catalán, C. Díaz, *Liebigs Ann. Rec.* **1997**, 1941 – 1949.
[49] G. Bourhill, J-L. Brédas, L-T. Cheng, S. R. Marder, F. Meyers, J. W. Perry, B. C. Tiemann, *J. Am. Chem. Soc.* **1994**, *116*, 2619 – 2620.
[50] C. Reichardt, *Chem. Rev.* **1994**, *94*, 2319 – 2358.
[51] J. Bañuelos Prieto, F. López Arbeloa, V. Martínez Martínez, T. Arbeloa López, F. Amat-Guerri, M. Liras, I. López Arbeloa, *Chem. Phys. Lett.* **2004**, *385*, 29 – 35.
[52] A. Dubois, M. Canva, A. Brun, F. Chaput, J. P. Boilot, *Appl. Opt.* **1996**, *35*, 3193 – 3199.
[53] W. Khon, A. D. Becke, R. G. Parr, *J. Phys. Chem.* **1996**, *100*, 12974 – 12980.
[54] A. D. Becke, *J. Chem. Phys.* **1996**, *104*, 1040 – 1046.
[55] C. Lee, W. Yang, R. G. Parr, *Phys. Rev. B* **1988**, *37*, 785 – 789.
[56] M. J. S. Dewar, E. G. Zoebish, E. F. Healy, J. J. P. Stewart, *J. Am. Chem. Soc.* **1985**, *107*, 3902 – 3909.
[57] M. J. Frisch, G. W. Trucks, H. B. Schlegel, G. E. Scuseria, M. A. Robb, J. R. Cheeseman, V. G. Zakrzewski, J. A. Montgomery, R. E. Stratmann, J. C. Burant, S. Dapprich, J. M. Millam, A. D. Daniels, K. N. Kudin, M. C. Strain, O. Farkas, J. Tomasi, V. Barone, M. Cossi, R. Cammi, B. Mennucci, C. Pomelli, C. Adamo, S. Clifford, J. W. Ochterski, G. A. Petersson, P. Y. Ayala, Q. Cui, K. Morokuma, D. K. Malick, A. D. Radbuck, K. Raghavachari, J. B. Foresman, J. Cioslowski, J.V. Ortiz, B. B. Stefanov, G. Liu, A. Liashenko, P. Piskorz, I. Komaromi, R. Gomperts, R. L. Martin, D. J. Fox, T. A. Keith,

  

M. A. Al-Laham, C. Y. Peng, A. Nanayakkara, C. Gonzalez, M. Challacombe, P. M. W. Gill, B. Johnson, W. Chen, M. W. Wong, J. L. Andres, M. Head-Gordon, E. S. Replogle, J. A. Pople, *Gaussian-98*, Gaussian Inc., Pittsburgh, PA, **1998**.

[58] J. J. P. Stewart, *MOPAC 2002*, Fujitsu Limited, Tokyo, Japan, **2001**.

[59] J. Baker, *J. Comput. Chem.* **1986**, *7*, 385 – 395.

[60] S. Hirata, T. J. Lee, M. Head-Gordon, *J. Chem. Phys.* **1999**, *111*, 8904 – 8912.

[61] M. A. Thompson, M. C. Zerner, *J. Am. Chem. Soc.* **1991**, *113*, 8210 – 8215.

Received: May 20, 2004
Revised: July 12, 2004

  